The Plant Cell, Vol. 11, 887–900, May 1999, www.plantcell.org © 1999 American Society of Plant Physiologists

Multicellular Compartmentation of *Catharanthus roseus* Alkaloid Biosynthesis Predicts Intercellular Translocation of a Pathway Intermediate

Benoit St-Pierre, Felipe A. Vazquez-Flota,[1] and Vincenzo De Luca[2,3]

Institut de Recherche en Biologie Végétale, Département de Sciences Biologiques, Université de Montréal, 4101 rue Sherbrooke est, Montréal, Québec H1X 2B2, Canada

In situ RNA hybridization and immunocytochemistry were used to establish the cellular distribution of monoterpenoid indole alkaloid biosynthesis in Madagascar periwinkle (*Catharanthus roseus*). Tryptophan decarboxylase (TDC) and strictosidine synthase (STR1), which are involved in the biosynthesis of the central intermediate strictosidine, and desacetoxyvindoline 4-hydroxylase (D4H) and deacetylvindoline 4-*O*-acetyltransferase (DAT), which are involved in the terminal steps of vindoline biosynthesis, were localized. *tdc* and *str1* mRNAs were present in the epidermis of stems, leaves, and flower buds, whereas they appeared in most protoderm and cortical cells around the apical meristem of root tips. In marked contrast, *d4h* and *dat* mRNAs were associated with the laticifer and idioblast cells of leaves, stems, and flower buds. Immunocytochemical localization for TDC, D4H, and DAT proteins confirmed the differential localization of early and late stages of vindoline biosynthesis. Therefore, we concluded that the elaboration of the major leaf alkaloids involves the participation of at least two cell types and requires the intercellular translocation of a pathway intermediate. A basipetal gradient of expression in maturing leaves also was shown for all four genes by in situ RNA hybridization studies and by complementary studies with dissected leaves, suggesting that expression of the vindoline pathway occurs transiently during early leaf development. These results partially explain why attempts to produce vindoline by cell culture technology have failed.

INTRODUCTION

The organs forming the plant body consist of several different cell types that are organized in relation to each other and that confer specific functions to the resulting organ. Each cell type emerges from an undifferentiated meristem according to a sophisticated and partially understood developmental program (Sylvester et al., 1996; von Arnim and Deng, 1996). The commitment to differentiate into specialized structures involves the perception by cells in the meristem of a complex array of signals, which communicate cellular age, position in relation to other cells, and hormonal balance. Environmental factors, such as light and temperature, also play a critical role in modulating these signals throughout the process of organogenesis (Bernier, 1988; Dale, 1988; Sylvester et al., 1996).

In addition to morphogenesis, developmental processes result in biochemical specialization of cells for the biosynthesis and/or accumulation of secondary metabolites, such as phenylpropanoids (Ibrahim et al., 1987; Reinold and Hahlbrock, 1997), monoterpenoids (Fahn, 1988; McCaskill et al., 1992), and alkaloids (Robinson, 1974, 1981; Nessler and Mahlberg, 1977; Eilert et al., 1985; Hashimoto and Yamada, 1994; Facchini and De Luca, 1995). Studies with germinating seedlings have suggested that alkaloid biosynthesis and accumulation are associated with seedling development (Weeks and Bush, 1974; De Luca et al., 1986; Aerts et al., 1994). Studies with mature plants also reveal this type of developmental control (Westekemper et al., 1980; Frischknecht et al., 1986). Furthermore, alkaloid biosynthesis in cell suspension cultures appears to be coordinated with cytodifferentiation (Kutchan et al., 1983; Lindsey and Yeoman, 1983).

Vindoline biosynthesis in *Catharanthus roseus* also appears to be under this type of developmental control (Westekemper et al., 1980; Constabel et al., 1982). In the leaves of *C. roseus*, vindoline is enzymatically coupled with catharanthine to produce the powerful cytotoxic dimeric alkaloids vinblastine and vincristine (Svoboda and Blake, 1975). Vindoline as well as the dimeric alkaloids are restricted to leaves and stems, whereas catharanthine is distributed equally throughout the aboveground and underground tissues (Westekemper et al., 1980; Deus-Neumann et al., 1987;

[1] Current address: Unidad de Biologia Experimental, Centro de Investigacion Cientifica de Yucatan, Apdo. Postal 87 Cordemex 97310 Merida, Yucatan, Mexico.

[2] Current address: Novartis Seeds Inc., Seed Biotechnology Research Unit, 3054 Cornwallis Road, Research Triangle Park, NC 27709.

[3] To whom correspondence should be addressed. E-mail vincenzo.de.luca@umontreal.ca; fax 514-872-9406.

Balsevich and Bishop, 1989). The developmental regulation of vindoline biosynthesis has been well documented in *C. roseus* seedlings, in which it is light inducible. This is in contrast to catharanthine, which also accumulates in etiolated seedlings (Balsevich et al., 1986; De Luca et al., 1986). Furthermore, cell cultures that accumulate catharanthine but not vindoline (van der Heijden et al., 1989) recover this ability upon redifferentiation of shoots (Constabel et al., 1982). These observations suggest that the biosynthesis of catharanthine and vindoline is differentially regulated and that vindoline biosynthesis is under more rigid tissue-, development-, and environment-specific control than is that of catharanthine.

More than 100 *C. roseus* alkaloids that have been identified share many common biosynthetic steps. The early stages of alkaloid biosynthesis in *C. roseus* involve the formation of tryptamine from tryptophan and its condensation with secologanin to produce the central intermediate strictosidine, the common precursor for the monoterpenoid indole alkaloids (Figure 1). The enzymes catalyzing these two reactions are tryptophan decarboxylase (TDC) and strictosidine synthase (STR1), respectively (reviewed in De Luca, 1993). Strictosidine is the precursor for both the *Iboga* (catharanthine) and *Aspidosperma* (tabersonine and vindoline) types of alkaloids (Figure 1). According to this biosynthetic scheme, further enzymatic reactions would transform tabersonine into vindoline, including hydroxylation at C-16, 16-*O*-methylation, hydration of the 2,3-double bond, *N*-methylation, hydroxylation at C-4, and 4-*O*-acetylation (De Luca et al., 1986, 1988). The first pair of reactions are catalyzed by tabersonine 16-hydroxylase and *S*-adenosyl-L-methionine:16-hydroxytabersonine-*O*-methyltransferase, respectively (St-Pierre and De Luca, 1995). The third to the last reaction is catalyzed by an *S*-adenosyl-L-methionine:2,3-dihydro-3-hydroxytabersonine-*N*-methyltransferase (De Luca et al., 1987; Dethier and De Luca, 1993), whereas 4-hydroxylation is catalyzed by desacetoxyvindoline 4-hydroxylase (D4H), a 2-oxoglutarate–dependent dioxygenase (De Carolis et al., 1990; De Carolis and De Luca, 1993). The final reaction is catalyzed by acetyl coenzyme A (CoA):deacetylvindoline 4-*O*-acetyltransferase (DAT; De Luca et al., 1985; Power et al., 1990). Some of these enzymes are not expressed in cell cultures or in tissues unable to produce vindoline (De Luca et al., 1986, 1988; De Carolis et al., 1990).

It has been suggested that certain tissues are required for alkaloid biosynthesis and/or accumulation. Yoder and Mahlberg (1976) used chemical indicators to identify laticifers and "specialized parenchyma cells" as the sites of alkaloid accumulation in *C. roseus.* Latex could be collected from *C. roseus* fruits and was shown to contain various monoterpenoid indole alkaloids (Eilert et al., 1985). Direct observation of *C. roseus* leaves by epifluorescence microscopy showed the random distribution of cells throughout the mesophyll that displayed distinctive autofluorescent properties (Mersey and Cutler, 1986). Leaf sections and protoplast preparations revealed the presence of larger yellow autofluorescent cells with few chloroplasts, compared with the surrounding red autofluorescent mesophyll cells. These "idioblast" cells (Mersey and Cutler, 1986), which occur in several plant families, are probably morphologically related to laticifers (Fahn, 1988), and they may be associated with the biosynthesis and accumulation of secondary products (Postek and Tucker, 1983; Platt and Thomson, 1992).

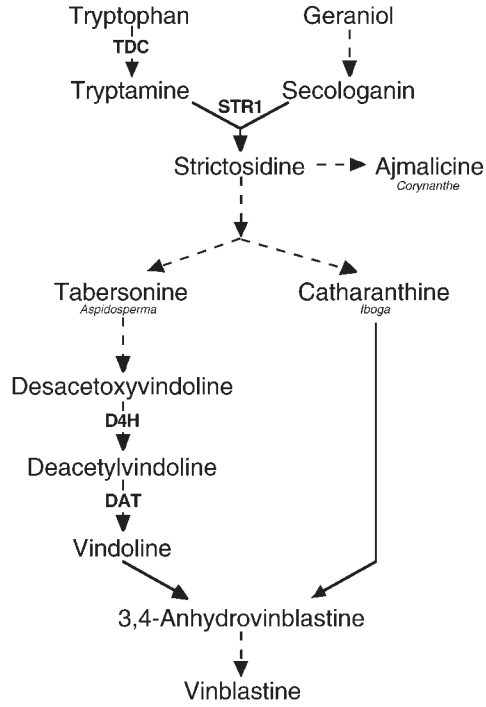

Figure 1. Terpenoid Indole Alkaloid Biosynthetic Pathway in *C. roseus*.

TDC converts tryptophan to tryptamine, and several enzymes convert geraniol into secologanin. STR1 converts tryptamine and secologanin into the central intermediate strictosidine, from which are derived the *Iboga*, *Corynanthe*, and *Aspidosperma* alkaloids, such as ajmalicine, catharanthine, and vindoline, respectively. The condensation of vindoline and catharanthine leads to the biosynthesis of the bisindole alkaloid vinblastine. Single and multiple enzymatic steps are shown as solid and dashed arrows, respectively.

In this study, we have used in situ RNA hybridization and immunocytochemistry to localize the cell-specific expression of *tdc*, *str1*, *d4h*, and *dat* in different tissues of *C. roseus* plants. The results suggest that the early (TDC and STR1) and late (D4H and DAT) reactions of vindoline biosynthesis occur in different cells.

RESULTS

Previous studies with *C. roseus* have illustrated that genes involved in indole alkaloid biosynthesis are preferentially ex-

pressed in young actively growing tissues. Very young leaves were fixed, embedded, sectioned, and prepared for in situ RNA hybridization studies to localize transcripts of *tdc*, *str1*, *d4h*, and *dat*, which catalyze early (*tdc* and *str1*) and late (*d4h* and *dat*) steps in vindoline biosynthesis, respectively (Figure 1). The longitudinal section of a young leaf (Figure 2, diagram at top) shows that the basal end is curled and suggests that cell expansion leading to leaf uncurling has yet to be completed because the bases of angiosperm leaves are developmentally younger than are the more distal parts.

C. roseus has simple, elliptical mesomorphic leaves (Mersey and Cutler, 1986) that are composed of several types of cells. The upper and lower epidermis are composed of thin-walled cells arranged in a single layer, whereas the mesophyll is arranged into a single layer of elongated palisade parenchyma on the adaxial side and a thicker multicellular spongy parenchyma on the abaxial side of the leaf (Figure 2). In addition, unbranched, nonarticulated laticifers are associated with the veins (Yoder and Mahlberg, 1976), which are curved and diverge from the midrib at a 35 to 45° angle (Mersey and Cutler, 1986). Branching from these are smaller veins generally composed of a tracheid and a laticifer. The palisade and spongy mesophyll also contain idioblasts, which can be identified by their distinctive yellow autofluorescence, when leaves are illuminated by blue light (Figures 3F and 3H), and by their distinctively larger size than surrounding mesophyll cells (Mersey and Cutler, 1986).

Cell-Specific Distribution of *tdc*, *str1*, *d4h*, and *dat* Transcripts in Developing Leaves

In situ RNA hybridizations of longitudinal sections with *tdc* and *str1* sense (Figures 2Q and 2R) and antisense (Figures 2A to 2H) transcripts revealed that expression of these two genes is completely restricted to the upper and lower leaf epidermis. In contrast, expression of *d4h* (Figures 2I to 2L) and *dat* (Figures 2M to 2P) mRNAs (cf. sense hybridization in Figures 2S and 2T to antisense hybridization in Figures 2I to 2P) is restricted almost exclusively to idioblasts occurring in the palisade and spongy mesophyll layers and to cross-connecting laticifers occurring at the interface between the palisade and spongy mesophyll. Cell-specific expression of each pair of transcripts was retained in the distal part of the leaf, but the levels of each transcript appeared to decrease with leaf maturation (cf. Figures 2B, 2F, 2J, and 2N with Figures 2C, 2D, 2G, 2H, 2K, 2L, 2O, and 2P). Visual inspection of Figure 2I suggests that *d4h* also is partially expressed in the upper epidermis of developmentally younger leaf tissue (Figures 2I and 2J), whereas it disappears in developmentally older upper epidermis while being retained in idioblasts and laticifers (Figures 2K and 2L).

Similar in situ RNA hybridization studies with older leaves also were performed (data not shown). Expression of all four genes decreased significantly in older leaves, but the same epidermis-, idioblast-, and laticifer-specific expression as in younger tissues was observed.

Laticifer- and Idioblast-Specific Expression of DAT

Fresh hand-cut longitudinal sections of young leaves were photographed under blue light illumination (390 to 490 nm). The upper epidermis, the lower epidermis, the yellow fluorescing cross-connecting laticifers with underlying tracheids, and the yellow fluorescing spongy mesophyll idioblast cells are clearly identified in the red fluorescent background of chlorophyll-rich mesophyll (Figure 3E). Palisade mesophyll–associated idioblasts, which also should display a yellow fluorescence, are not clearly identified in this longitudinal section, but many individual idioblasts are seen between cross-connecting laticifer cells on the adaxial face of *C. roseus* leaves (Figure 3F). Time-course studies have shown that the components that are responsible for the yellow fluorescence quickly diffuse from sectioned idioblast cells, which readily explains the lack of fluorescence observed for palisade mesophyll idioblasts in longitudinal leaf sections (Figure 3E). Longer incubation times also resulted in loss of the yellow fluorescent compounds occurring in laticifers (data not shown).

A comparison of longitudinal leaf sections hybridized with antisense *dat* probe (Figure 3A) to the hand-cut sections shows a clear correlation between the expression of *dat* and the greenish yellow fluorescence that is characteristic of laticifer and spongy mesophyll–associated idioblast cells (Figure 3E). This correlation also was demonstrated for palisade mesophyll–associated idioblast cells; their characteristic fluorescence is best viewed on the adaxial faces of a whole mount (Figure 3F). Additional in situ RNA hybridization studies were conducted with paradermal sections prepared by starting from the adaxial side of the leaves. Palisade mesophyll idioblasts and vasculature-associated laticifer cells are visualized first (Figure 3B), whereas cross-connecting laticifer cells become apparent in the paradermal section 20 μm further into the leaf (Figure 3C). The palisade mesophyll idioblasts (Figure 3B) can be distinguished from other palisade cells because of their larger size (Mersey and Cutler, 1986). The detection of *dat* transcripts within these cell types (Figures 3B and 3C) corroborates the results obtained from the analysis of longitudinal sections (Figures 2O and 3A). A magnified view (Figure 3D) of part of Figure 3C confirms the close relationship observed between the presence of *dat*-expressing laticifers and the underlying tracheids. This close relationship is clearly observed in the precise alignment of greenish yellow laticifers seen from the upper leaf surface (Figure 3F) with the vascular structures seen from the same surface cleared of pigments after treatment with organic solvents (Figure 3G). The abaxial side of the *C. roseus* leaf clearly reveals the greenish yellow fluorescence of spongy mesophyll–associated idioblast cells (Figure 3H) that also express *dat* (Figure 3A).

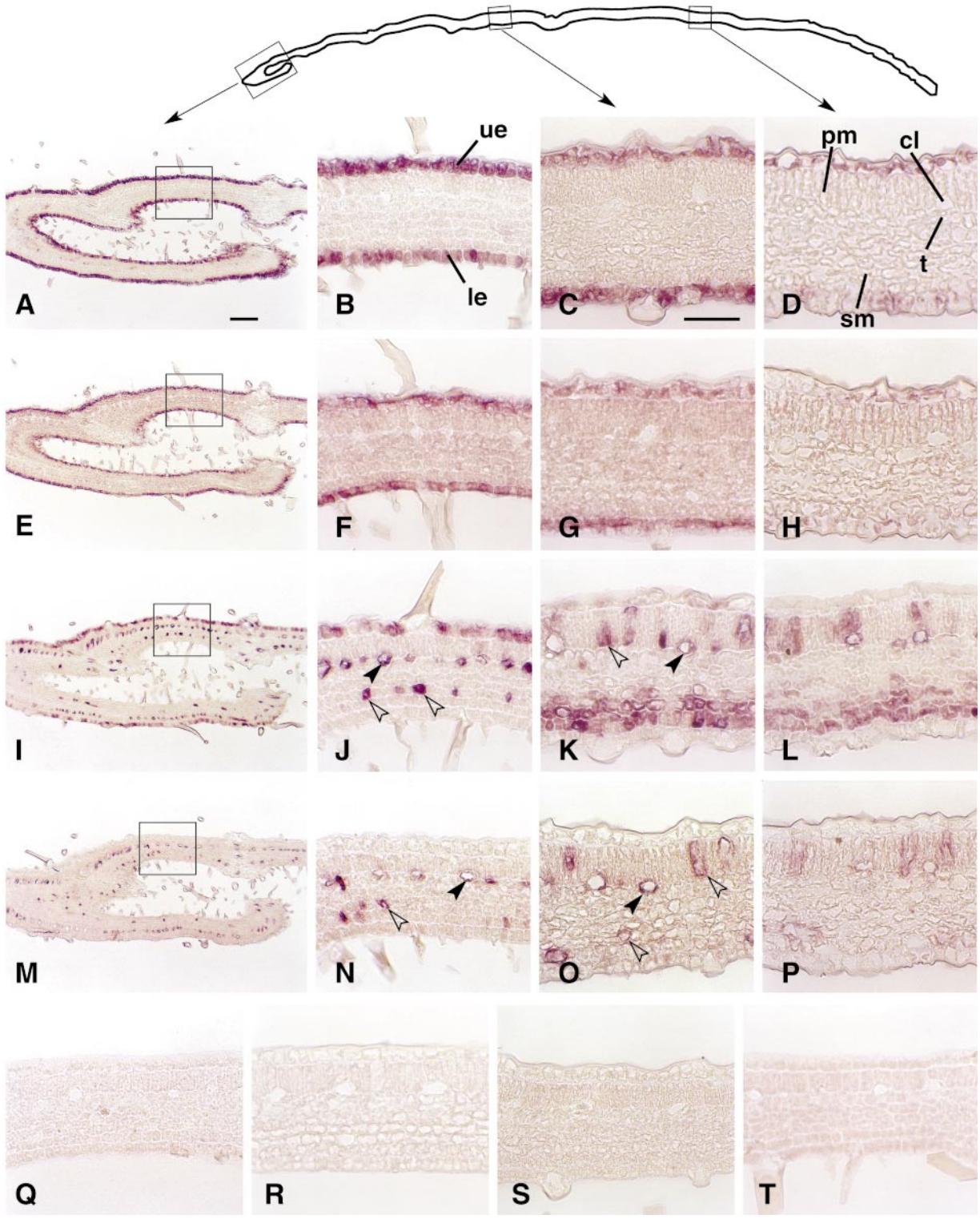

Figure 2. Localization of *tdc*, *str1*, *d4h*, and *dat* mRNA in Developing Leaves.

Paraffin-embedded serial longitudinal sections from 15-mm leaves were hybridized with digoxigenin-labeled transcripts. Hybridized transcripts were immunolocalized with anti-digoxigenin–alkaline phosphatase conjugate followed by BCIP/nitro blue tetrazolium color development. Boxes

Cell-Specific Distribution of TDC, D4H, and DAT Proteins in Developing Leaves

Longitudinal sections of the same *C. roseus* leaf shown in Figure 2 were treated with polyclonal rabbit antibodies raised against TDC (Fernandez et al., 1989), D4H (Vazquez-Flota and De Luca, 1998), and DAT (St-Pierre et al., 1998), respectively, to identify which leaf cells produce these proteins. Expression of the TDC protein is completely restricted to the upper and lower leaf epidermis (Figures 4A and 4B), as was the case for *tdc* transcript (Figures 2A to 2H). Similarly, expression of D4H (Figures 4C and 4D) and DAT (Figures 4E and 4F) proteins appeared to be restricted to idioblasts and laticifers, which are also the sites of expression for the respective mRNAs (Figures 2I to 2P). In contrast to the expression of *d4h* transcripts, which also was observed in the upper epidermis of developmentally younger leaf tissue in Figure 2I, the D4H protein was detected only in idioblasts and laticifers throughout the leaf section (Figures 4C and 4D; data not shown). Treatment of sections with preimmune serum did not produce any immune reactions to any cell type in these sections, even when applied at a low dilution (Figures 4G and 4H). Visual inspection of longitudinal sections also confirmed that the patterns of TDC, D4H, and DAT protein expression coincided with those of transcript accumulation and that the levels of each protein appeared to decrease with developmental age. The identical results obtained for the localization of *tdc*, *d4h*, and *dat* transcripts compared with TDC, D4H, and DAT proteins strongly suggest that at least two different cell types within the same tissue are involved in the biosynthesis of vindoline in *C. roseus*.

Differential Accumulation of TDC, STR1, D4H, and DAT in the Leaf Blade

Visual inspection of longitudinal sections of *C. roseus* leaves suggested that the leaf base contained the highest levels of all four mRNAs (Figure 2) and of the three enzymes (Figure 4). The middle portion of the leaf expressed lower levels of this pathway, whereas virtually no expression was observed near the tip of the leaf blade. These results suggest a basipetal gradient of expression for the genes involved in indole alkaloid biosynthesis. This pattern of expression also correlates with the denser distribution of laticifers characteristic for the basal area compared with those found in the middle section or at the tip of the leaf. It also correlates with a basipetal gradient of the yellow autofluorescent compounds in the laticifer and idioblast cells (result not shown).

To confirm this general trend, we dissected immature leaves (Figure 5, lower right) into base, middle, and tip areas to determine the levels of these four transcripts and of TDC, D4H, and DAT enzymes. RNA and protein were extracted separately from whole leaves or their components, as shown in Figure 5. RNA gel blot analysis (Figure 5, left) clearly showed the basipetal distribution of all four transcripts, with the highest, intermediate, and lowest levels occurring in the basal, middle, and tip regions of the leaf, respectively. However, immunoblot analysis (Figure 5, right) revealed that the levels of the three proteins were almost equivalent in the basal and middle regions of the leaves. Their levels declined only in the tip region of the leaf, suggesting that these proteins were more stable than were their corresponding mRNAs during leaf maturation. These results, which clearly suggest that the pathway leading to vindoline biosynthesis appears very early in leaf development, corroborate the qualitative differences in the levels of the corresponding transcripts as observed by in situ RNA hybridization of *C. roseus* leaves (Figure 2).

Sites of Indole Alkaloid Biosynthesis in Flower Primordia, Stems, and Roots Tips

Previous studies using various techniques have demonstrated that most *C. roseus* tissues are active in the biosynthesis of indole alkaloids and that each organ accumulates a characteristic spectrum of alkaloids. In situ RNA hybridization studies were conducted to identify which cells in developing flowers, stems, and root tips actually were involved in

Figure 2. (continued).

in the profile of a longitudinal section at the top show the photographed area: the revoluted leaf base (first box; **[A]**, **[E]**, **[I]**, and **[M]**), the middle area of the leaf at a distance of 4.5 mm from the base (second box; **[C]**, **[G]**, **[K]**, and **[O]**), and the tip portion of the leaf at 8.5 mm from the base (third box; **[D]**, **[H]**, **[L]**, and **[P]**). Boxed areas in **(A)**, **(E)**, **(I)**, and **(M)** are magnified in **(B)**, **(F)**, **(J)**, and **(N)**, respectively. A magnification of the leaf base also is shown in **(Q)** to **(T)**.

(A) to **(D)** Sections were hybridized with antisense RNA for *tdc*.

(E) to **(H)** Sections were hybridized with antisense RNA for *str1*.

(I) to **(L)** Sections were hybridized with antisense RNA for *d4h*.

(M) to **(P)** Sections were hybridized with antisense RNA for *dat*.

(Q) to **(T)** Sections were hybridized with sense RNA for *tdc* **(Q)**, *str1* **(R)**, *d4h* **(S)**, and *dat* **(T)**.

cl, cross-connecting laticifer cells; le, lower epidermis; pm, palisade mesophyll cells; sm, spongy mesophyll cells; t, tracheid; ue, upper epidermis. Solid arrowheads show laticifer cells; open arrowheads point to idioblast cells. Bar in **(A)** = 100 μm for panels **(A)**, **(E)**, **(I)**, and **(M)**; bar in **(C)** = 50 μm for **(B)** to **(D)**, **(F)** to **(H)**, **(J)** to **(L)**, and **(N)** to **(T)**.

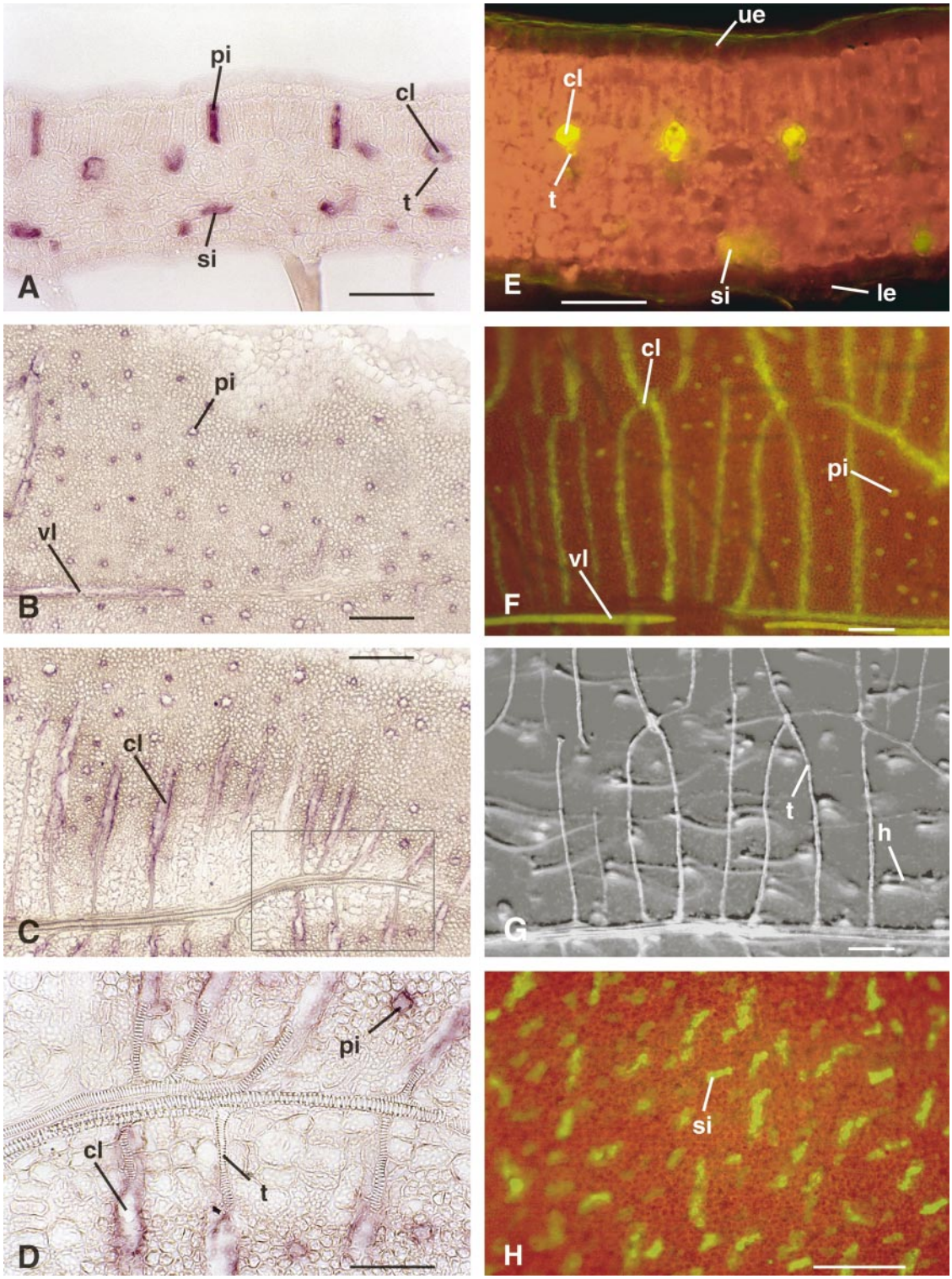

Figure 3. Localization of *dat* mRNA, Fluorescent Compounds, and Vascular Tissue in Developing Leaves.

(A) to **(D)** Paraffin-embedded sections were hybridized with antisense RNA for *dat*. **(A)** shows a longitudinal section of the leaf base, **(B)** a paradermal section mainly through the palisadic mesophyll, **(C)** a paradermal section 20 μm under the section shown in **(B)**, and **(D)** magnification of the boxed area shown in **(C)**.

alkaloid biosynthesis. Serial longitudinal sections of flower buds (Figures 6A, 6D, 6G, and 6J) clearly demonstrate that both *tdc* and *str1* transcripts are expressed only in the epidermis of developing flower petals and sepals, whereas the expression of *d4h* and *dat* is restricted to laticifer cells. Stem cross-sections, which were obtained from the first internode under the youngest developing leaves, also displayed a pattern of gene expression (Figures 6B, 6E, 6H, and 6K) identical to that of developing flowers (Figures 6A, 6D, 6G, and 6J) and leaves (Figures 2 and 3). Expression of *tdc* and *str1* transcripts is restricted to stem epidermis (Figures 6B and 6E), whereas both *d4h* and *dat* transcripts are clearly expressed in subdermal laticifers and in vasculature-associated laticifers (Figures 6H and 6K).

Serial longitudinal sections of root tips (Figures 6C, 6F, 6I, and 6L) also were studied for the presence of each of these transcripts. Expression of both *tdc* and *str1* is restricted to protodermal and cortical cells along most of the longitudinal sections, but it appears to decrease in older developmental stages (Figures 6C and 6F). The root cap and the stele do not appear to express either of these mRNAs. It is not surprising that neither *d4h* (Figure 6I) nor *dat* (Figure 6L) transcripts are expressed in root tips, because roots do not express the late stages of vindoline biosynthesis.

The cellular distribution of TDC, D4H, and DAT antigens also was studied in flower buds, stems, and root sections (data not shown). The results obtained clearly corroborate those of the in situ RNA hybridization studies reported in Figure 6.

DISCUSSION

We have demonstrated the cell type–specific localization of enzymes involved in steps in indole alkaloid biosynthesis in *C. roseus* that are common to all *C. roseus* alkaloids (TDC and STR1) and in steps comprising the vindoline-specific branch of the pathway (D4H and DAT). One striking observation was the coordinate regulation observed for both the common and vindoline-specific branch of the pathway. For instance, the mRNA distribution patterns for both *tdc* and *str1* were identical within different tissues and developmental stages. Expression of *tdc* and *str1* was restricted to the epidermis of leaves, stems, and flowers (Figures 2A to 2H, 6A, 6B, 6D, and 6E). In contrast, expression of *tdc* and *str1* in roots was restricted to the cortical and protodermal cells of the root apex (Figures 6C and 6F). It was shown previously that the distribution in various organs and induction kinetics of *tdc* and *str1* mRNAs under various conditions were strictly coordinated (Pasquali et al., 1992). This study reveals that coordinate regulation of these genes is associated with cell type–specific and developmental control.

The genes representing the late stage of vindoline biosynthesis also were expressed, at least at the protein level, in the same cell type. D4H and DAT proteins were associated with laticifers and idioblasts of leaves (Figure 4C to 4F), stems, and flowers (results not shown). *d4h* and *dat* mRNAs also were colocalized in idioblast and laticifer cells of leaves, stems, and flower buds (Figures 2I to 2P, 6G, 6H, 6J, and 6K), and there was no detectable expression of either gene in roots (Figures 6I and 6L). However, ectopic accumulation of *d4h* mRNA was observed in upper epidermal cells and in some spongy mesophyll cells in the vicinity of idioblast cells (Figures 2I to 2L) without the concomitant accumulation of D4H protein (Figures 4C and 4D). Whereas coordinate regulation of *d4h* and *dat* was expected from many lines of evidence, particularly from their induction kinetics and light-dependent regulation in developing seedlings, as well as their distribution patterns in mature plants, some data suggested specific mechanism of regulation for *d4h*. For instance, *d4h* mRNAs (Vazquez-Flota and De Luca, 1998), in contrast to those of *dat* (St-Pierre et al., 1998), rose to significant levels in dark-grown seedlings.

The in situ RNA hybridization and immunocytochemical localization studies presented in this report revealed that expression of the vindoline pathway follows a basipetal distribution in young expanding leaves (Figures 2 and 4). These results were confirmed by immunoblot and RNA blot analysis of dissected leaf segments (Figure 5). This expression pattern suggests activation of the vindoline pathway genes in young immature leaf tissues and rapid downregulation with tissue maturation. In dicots, cell division frequently occurs until the lamina has reached ~90% of its final leaf area (Dale, 1988). The young leaves used in this study were 20% of their final, mature, fully expanded size and were therefore probably undergoing active cell division. However, the basal region appears to undergo a more active cell division than does the leaf tip, where cells are more developmentally mature and cellular volume increase is the more predominant growth process (Dale, 1988). The distribution of gene expression observed confirms that alkaloid biosynthesis is initiated in very young rapidly growing tissues. The accumulation of alkaloids in such tissues may be a defensive and

Figure 3. (continued).

(E) to **(H)** Reflected light fluorescence microscopy (**[E], [F]**, and **[H]**) of fresh tissues and cross-illumination microscopy of cleared tissues **(G)**. Shown are fresh hand-cut cross-sections **(E)**, adaxial and abaxial face of whole mount (**[F]** and **[H]**, respectively), and vascular tissue of the leaf section **(G)** shown in **(F)** after clearing of the tissues. cl, cross-connecting laticifer cells; h, trichome; le, lower epidermis; pi, palisade mesophyll–associated idioblast cells; si, spongy mesophyll–associated idioblast cells; t, tracheid; ue, upper epidermis; vl, vasculature-associated laticifer cells. Bars in **(A)** and **(D)** = 50 μm; bars in **(B)**, **(C)**, and **(E)** to **(H)** = 100 μm.

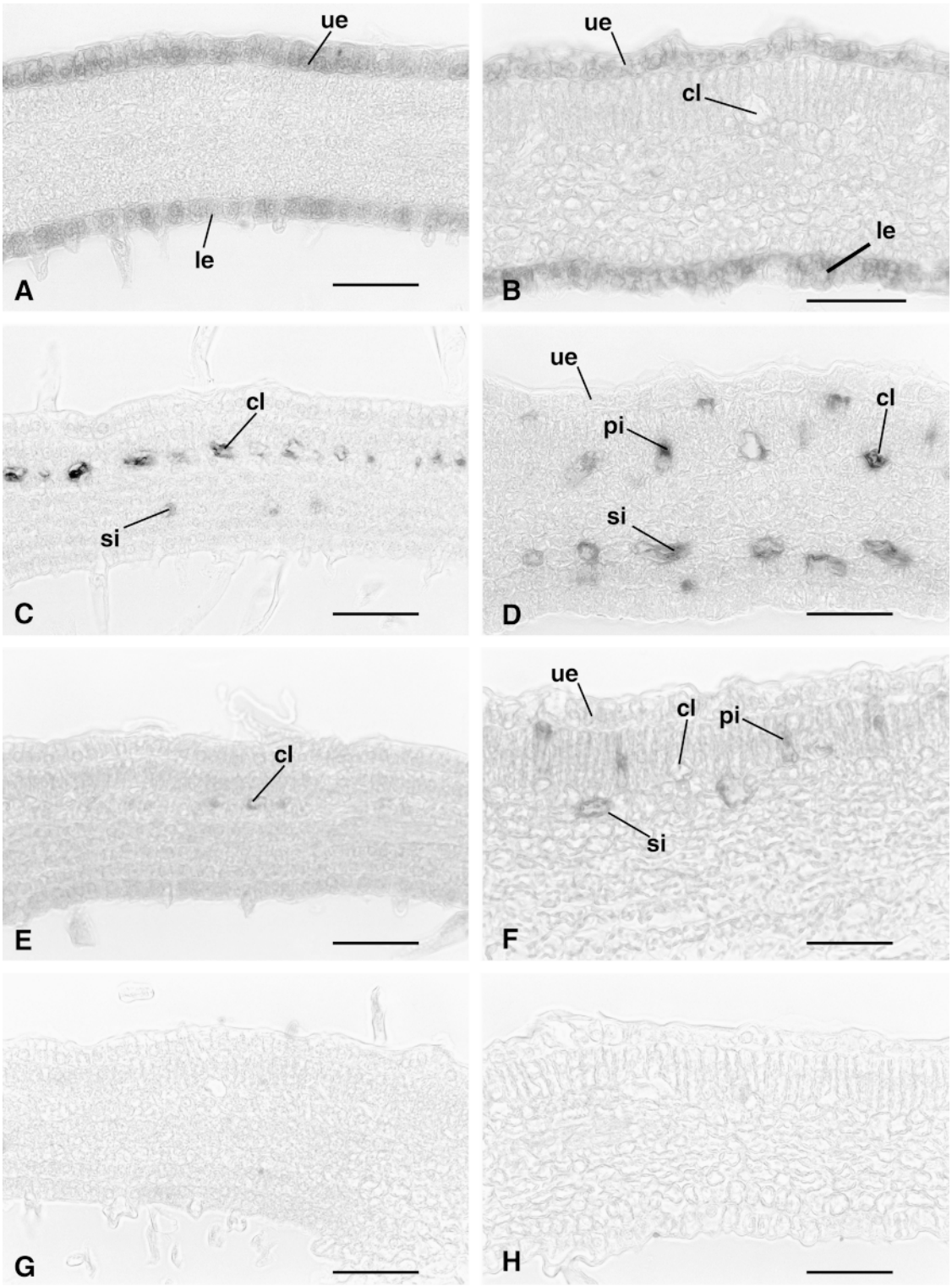

Figure 4. Immunolocalization of TDC, D4H, and DAT Proteins in Developing Leaves.

Longitudinal sections of the same leaf shown in Figure 2. Microscopy is from the base (**[A]**, **[C]**, **[E]**, and **[G]**) and from the middle portion (4.5 mm from the base) of the leaf (**[B]**, **[D]**, **[F]**, and **[H]**).

protective strategy against predators (Luijendijk et al., 1996). Some antifeedant properties have been associated with vindoline accumulation (G. Guillet, F.A. Vazquez-Flota, and V. De Luca, unpublished results), and the cytotoxic effects of the dimeric alkaloids also point to such a role. However, the bisindole alkaloids generally are absent in young shoots (Balsevich and Bishop, 1989), suggesting that the ability to synthesize and accumulate dimers appears with leaf maturation.

The studies also revealed a spatial separation of the vindoline pathway within particular cells in leaf, stem, and flower tissues (Figures 2, 4, and 6). These results indicate that the early vindoline pathway is restricted to the epidermal layers of immature leaves and stems, whereas the late steps committed exclusively to vindoline formation are located in laticifers and idioblasts. This raises questions about the number of pathway steps occurring in the epidermis and how specific intermediates are mobilized into laticifers and idioblasts for elaboration into vindoline.

Tabersonine and post-tabersonine intermediates have been detected in *C. roseus* roots (Svoboda and Blake, 1975) as well as in hairy root and laticiferless (Eilert et al., 1985) cell cultures (Toivonen et al., 1989; van der Heijden et al., 1989; Bhadra et al., 1993). These results suggest that laticifers are not required for tabersonine biosynthesis. However, the ability of stem and leaf epidermis to participate in alkaloid biosynthesis suggests but does not prove that tabersonine could be made in the epidermis. Tabersonine or a later intermediate then could be the transport form, which is translocated to laticifers and idioblasts for enzymatic elaboration into vindoline. Cell-to-cell mobilization has been well documented for flavonoids in parsley plants (Reinold and Hahlbrock, 1997). Because laticifers are closely associated with the vascular system of the plant (Figure 3), transport of vindoline pathway intermediates from roots also seems possible.

The role of laticifers and idioblasts in the terminal steps of vindoline biosynthesis raises the question of where the biochemical coupling of vindoline and catharanthine to make highly toxic indole alkaloid dimers occurs. It is conceivable that these specialized cells are required to accommodate and sequester the toxic dimers from normal cellular processes.

The participation of separate organs and/or cells in the synthesis and accumulation of secondary metabolites appears to be a common characteristic in plants. For example, nectaries, trichomes, and other secretory structures that originate from epidermal cells (Fahn, 1988) represent major sites of synthesis for various terpenoids (Keene and Wagner, 1985). Expression of phenylalanine ammonia–lyase (*pal*) and chalcone synthase (*chs*), which are involved in flavonoid biosynthesis, also has been localized in epidermal cells (Reinold and Hahlbrock, 1997). The reciprocal grafting between nicotine-producing and nonproducing tobacco plants showed that this alkaloid is synthesized mainly in roots and is then translocated via xylem to the leaves (reviewed in Hashimoto and Yamada, 1994). Similarly, the localization of hyoscyamine 6β-hydroxylase in the pericycle of young roots of *Hyoscyamus niger* revealed that hyoscyamine is converted to scopolamine in roots before its translocation to stems and leaves for final storage (Hashimoto and Yamada, 1994). In opium poppy, the first committed step in the synthesis of the morphine-type and other benzylisoquinoline alkaloids involves the decarboxylation of tyrosine by tyrosine decarboxylase (TyDC). Transcripts of the different members of the *tydc* gene family were detected mainly in the vascular tissues (metaphloem and protoxylem) of young stems and roots

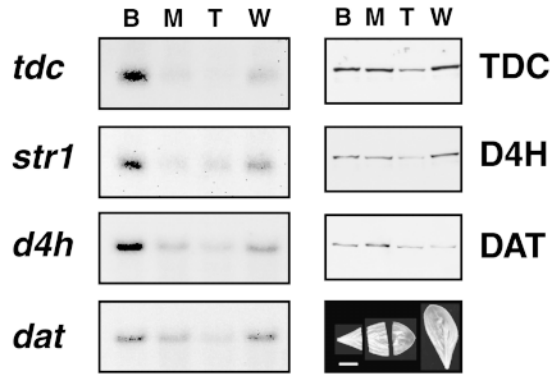

Figure 5. Distribution of Protein and mRNA for Alkaloid Biosynthetic Genes in Dissected Developing Leaves.

Whole leaves (W) and leaves that were dissected into base (B), middle (M), and tip (T) regions, as shown at lower right, were analyzed for antigen levels (right) of TDC, D4H, and DATand RNA levels (left) of *tdc*, *str1*, *d4h*, and *dat.* Bar = 5 mm.

Figure 4. (continued).

(A) and **(B)** Leaf section reacted with the TDC antiserum (1:1000).
(C) and **(D)** Leaf section reacted with the D4H antiserum (1:2500).
(E) and **(F)** Leaf section reacted with the DAT antiserum (1:400).
(G) and **(H)** Leaf section reacted with the preimmune antiserum (1:500).
Abbreviations are the same as given for Figure 3. Bars in **(A)** to **(H)** = 50 μm.

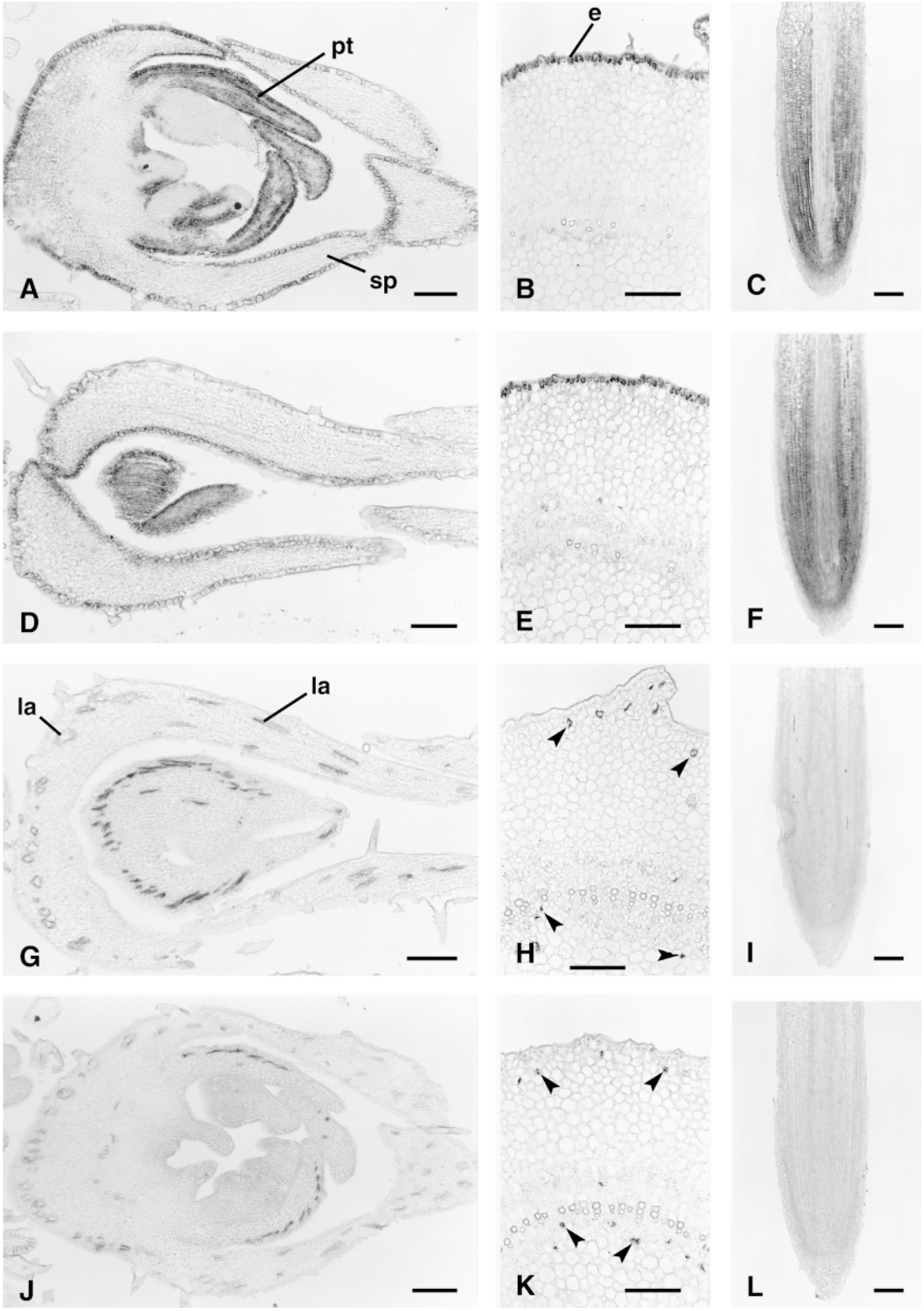

Figure 6. Localization of *tdc*, *str1*, *d4h*, and *dat* mRNA in Flower Primordia, Stems, and Roots.

(Facchini and De Luca, 1995). The present study suggests that the precise cell-, tissue-, and organ-specific compartment of monoterpenoid indole alkaloid biosynthesis, and of secondary metabolism in general, is regulated by differential expression of biosynthetic pathways and by a controlled transport of intermediates to the most appropriate sites for accumulation.

It is not clear if a similar root-to-shoot alkaloid transport system exists in *C. roseus.* Catharanthine and advanced precursors of vindoline biosynthesis, such as tabersonine, may be synthesized in roots to be transported to laticifers and idioblasts in leaves and stem, for elaboration into dimeric alkaloids and vindoline, respectively. However, the ability of in vitro leaf cultures, which have no roots, to make vindoline suggests that roots are not absolutely required to make this possible (Endo et al., 1987). The available evidence suggests that tabersonine and catharanthine may be produced in more than one location, and it remains to be elucidated how substrates for vindoline and dimer production are made available.

The clear differential cell localization of the early and late stages of vindoline biosynthesis in leaves strongly suggests that undetermined poststrictosidine compounds are mobilized from the epidermis to laticifers and idioblasts, where at least the last two reactions of vindoline biosynthesis take place. Differential cell-specific expression and intercellular transport of metabolites also have been suggested for the phenylpropanoid pathway (Reinold and Hahlbrock, 1997). In parsley leaves, the genes involved in general phenylpropanoid metabolism, such as *pal* and 4-coumarate:CoA ligase (*4cl*), are expressed mainly in the vascular bundle and in epithelial cells surrounding oil ducts. Lower levels of *pal* and *4cl* transcripts also were detected in the leaf epidermis, palisade cells, and spongy mesophyll cells and within the oil duct surrounding cells (Reinold and Hahlbrock, 1997).

However, the locations of the pathways leading to the formation of flavonoids or furanocoumarins were mutually exclusive. Flavonoids and furanocoumarins are two major products derived from different branches of the phenylpropanoid pathway, downstream from 4-coumaryl–CoA. *chs*, which is involved specifically in flavonoid biosynthesis, was restricted to the epidermis, spongy mesophyll, and oil duct surrounding cells. *S*-adenosyl-L-methionine:bergaptol *O*-methyltransferase, which is involved in furanocoumarin biosynthesis, occurred in the vascular bundle, palisade parenchyma, and the oil duct epithelial cells (Reinold and Hahlbrock, 1997). Interestingly, flavonoids were detected in vascular bundles and oil duct epithelial cells that do not express *chs*, suggesting the mobilization of these compounds from other expressing cells (Reinold and Hahlbrock, 1997).

A similar cellular distribution to those of leaves also was found for TDC, STR1, and D4H (F.A. Vazquez-Flota, B. St-Pierre, and V. De Luca, manuscript in preparation) in cotyledons of developing seedlings. No differences in the cellular distribution of D4H were found in the cotyledons of dark- or light-grown seedlings. The presence of inactive D4H protein in idioblasts and laticifers of etiolated seedlings indicates that this isoform of D4H is expressed properly in laticifers and idioblasts from the early stages of seedling development. The results suggest that light activates *d4h* and *dat* expression (F.A. Vazquez-Flota, B. St-Pierre, and V. De Luca, manuscript in preparation) rather than inducing the production of particular cells, such as idioblasts or laticifers. It remains to be established, however, whether light triggers the formation/proliferation of particular subcellular structures required for vindoline biosynthesis.

Because no clear physiological roles for vindoline have been described, this alkaloid could be considered both as a final product as well as a precursor in the formation of the dimeric alkaloids. In the latter event, the suggested spatially separate origin of the catharanthine subunit may play a critical role in regulating the formation of dimers, which have been shown to be toxic when applied to cell suspensions of *C. roseus* (V. De Luca, unpublished results).

The distribution of *tdc* and *str1* in actively growing shoots and roots of *C. roseus* plants (Figures 2 and 6; Fernandez et al., 1989) suggests that the meristems of different organs are capable of making tryptamine and monoterpenoid indole alkaloids. The actual presence of different alkaloids in both aboveground and underground tissues suggests that distinct tissue-specific biosynthetic pathways are expressed. High levels of catharanthine have been found in roots of mature plants, whereas shoots, which accumulate lower levels of catharanthine, appear to be the exclusive sites of vindoline accumulation (Westekemper et al., 1980; Deus-Neumann et al., 1987). This conclusion is clearly supported by the flower bud–, leaf-, and stem-specific distribution of *d4h* and *dat* (Figures 2 and 6).

Figure 6. (continued).

Serial longitudinal sections of flower buds (**[A]**, **[D]**, **[G]**, and **[J]**) and root apices (**[C]**, **[F]**, **[I]**, and **[L]**) and cross-sections of first internodes under the youngest developing leaf (**[B]**, **[E]**, **[H]**, and **[K]**) were hybridized with digoxigenin-labeled transcripts.

(A) to **(C)** Sections were hybridized with antisense RNA for *tdc.*

(D) to **(F)** Sections were hybridized with antisense RNA for *str1.*

(G) to **(I)** Sections were hybridized with antisense RNA for *d4h.*

(J) to **(L)** Sections were hybridized with antisense RNA for *dat.*

e, epidermal cells; la, laticifer cells; pt, petals; sp, sepals. Arrowheads point to laticifer cells in stem. Bars in **(A)** to **(L)** = 100 μm.

METHODS

Tissue Fixation and Embedding

Tissue samples from mature *Catharanthus roseus* plants were infiltrated in vacuo in FAA (50% ethanol, 5% acetic acid, and 5% formaldehyde) for 30 min and transferred to fresh FAA at 4°C for 16 hr. After ethanol and *tert*-butanol series, the samples were incubated overnight at 60°C, first in Paraplast:*tert*-butanol (1:1) and then in pure Paraplast (Oxford Labware, St. Louis, MO). The Paraplast-embedded samples were sectioned to a thickness of 10 μm by using a rotary microtome. Sections were spread on slides pretreated with 2% (v/v) 3-aminopropyltriethoxysilane (Sigma) in acetone, dried for 24 hr at 40°C, and stored until use. Two 15-min incubations in xylene were used to remove paraffin from the samples, and an ethanol series up to water was used to rehydrate the sections.

In Situ RNA Hybridization

The following plasmids were used for generating sense and antisense RNA probes. All inserts were in pBluescript SK− or SK+ (Stratagene, La Jolla, CA). For tryptophan decarboxylase (*tdc*), pTDC5 contains a 1.7-kb full-length cDNA fragment (De Luca et al., 1989). For strictosidine synthase *(str1)*, a 0.9-kb fragment from the *str1* cDNA clone (McKnight et al., 1990) was subcloned into pBluescript SK+. For desacetoxyvindoline 4-hydroxylase (*d4h*), cD4H-3A contains a 1.2-kb fragment of *d4h* cDNA (Vazquez-Flota et al., 1997). For deacetylvindoline 4-*O*-acetyltransferase (*dat*), pBSDAT3 contains a 1.3-kb fragment representing the coding region of *dat* obtained by polymerase chain reaction amplification of *gDAT-6* (St-Pierre et al., 1998). RNA probes were synthesized by in vitro transcription with digoxigenin–UTP and T7 or T3 RNA polymerase, according to the manufacturer's instructions (Boehringer Mannheim). RNA probes were submitted to partial alkaline hydrolysis for 20 min at 60°C (Jackson, 1992).

Rehydrated sections were prepared for in situ hybridization by treatment with proteinase K (2 μg/mL in 100 mM Tris-HCl and 50 mM EDTA, pH 8.0) for 30 min at 37°C, followed by two rinses with TBS buffer (150 mM NaCl and 10 mM Tris-HCl, pH 7.5), by blocking of proteinase K with glycine (2 mg/mL in TBS) for 2 min, and by two rinses in TBS buffer. Sections were postfixed with 3.7% formaldehyde in PBS buffer for 20 min and washed in TBS for 5 min. Finally, sections were acetylated with acetic anhydride (0.25% in 0.1 M triethanolamine–HCl, pH 8.0) for 10 min, washed with TBS, dehydrated in an ethanol series, and air dried.

For hybridization, portions of hybridization mixture (60 μL) were dispersed on a cover slip (22 × 50 mm), and the slides were inverted onto the droplet of probe. Hybridization mixture included 200 ng/mL of hydrolyzed digoxigenin–labeled RNA transcripts, 40% formamide, 10% dextran sulfate, 1 mg/mL yeast tRNA, 0.5 mg/mL polyadenylic acid, 0.3 M NaCl, 0.01 M Tris-HCl, pH 6.8, 0.01 M Na phosphate, pH 6.8, 5 mM EDTA, and 40 units per mL RNasin ribonuclease inhibitor (Promega). Hybridization was for 16 to 18 hr at 50°C in an atmosphere of 50% formamide. Cover slips were then detached by soaking in 2 × SSC at 37°C (1 × SSC is 0.15 M NaCl and 0.015 M sodium citrate). Slides were treated with RNase A (50 μg/mL in 0.5 M NaCl, 10 mM Tris-HCl, pH 7.5, and 1 mM EDTA) for 30 min at 37°C and then washed in 2 × SSC for 1 hr, in 1 × SSC for 1 hr, and in 0.1 × SSC for 1 hr at 65°C.

For immunolocalization of hybridized transcripts, slides were washed in TBST (0.1 M Tris-HCl, pH 8.0, 0.15 M NaCl, and 0.3% Triton X-100) for 10 min and blocked with 2% BSA fraction V (Boehringer Mannheim) in TBST for 16 hr at 4°C. Portions (60 μL) of sheep anti-digoxigenin–alkaline phosphatase conjugate (Boehringer Mannheim) at a 1:200 dilution in a solution of 1% BSA in TBST were dispensed onto cover slips, and the slides were inverted onto the droplet. After a 2-hr incubation at room temperature, the unbound conjugates were washed twice for 15 min with TBST and twice for 10 min with AP buffer (0.1 M Tris-HCl, pH 9.5, 0.1 M NaCl, and 10 mM $MgCl_2$). For color development, slides were immerged in 175 μg/mL 5-bromo-4-chloro-3-indolyl phosphate (BCIP) and 350 μg/mL nitro blue tetrazolium chloride in AP buffer for 8 to 10 hr at 22°C. After development, slides were washed in water and mounted with 50% glycerol, 7% gelatin, and 1% phenol and covered with a cover slip.

Immunocytochemical Localization of TDC, D4H, and DAT

For immunolocalization of proteins, sections were rehydrated, as described above, washed in TBSW (10 mM Tris-HCl, pH 7.5, 150 mM NaCl, and 0.05% Tween 20) for 10 min, and treated with blocking solution (3% BSA in TBSW) for 16 hr at 4°C. After washing with TBSW, sections were incubated with primary crude antisera diluted with blocking solution (see legend to Figure 4) for 2 to 4 hr at room temperature in a humid chamber. After four 15-min washes in TBSW, the sections were incubated with goat anti–rabbit IgG–alkaline phosphatase conjugate (Bio-Rad) at a 1:1000 dilution in blocking solution. After a 2-hr incubation at room temperature, unbound conjugates were washed twice for 15 min with TBSW and twice for 15 min with carbonate buffer (100 mM $NaHCO_3$, pH 9.8, and 1 mM $MgCl_2$). The slides were immerged with 150 μg/mL BCIP and 300 μg/mL nitro blue tetrazolium chloride in carbonate buffer for 1 hr at 22°C.

Fluorescence Microscopy

Fresh hand-cut sections of developing leaves were observed by a reflected light fluorescence microscope (model BH-2 RFCA; Olympus Optical Co., Tokyo, Japan), equipped with blue excitation (wide band) dichroic mirror/filter combination, and photographed with Kodak Ektachrome 400X film (Kodak Canada, Toronto, Canada). The intensity of the green channel of the images in RGB (red green blue) mode was enhanced with Photoshop 3.0. After clearing of the tissue with Herr's buffer (Herr, 1971), the leaf vascular tissue was observed by using an Olympus microscope whose bright-field condenser (BH2-UCD) position was off axis. The magenta channel of the image in CMYK mode was converted to a grayscale image.

Protein and RNA Gel Blot Analysis

Proteins were extracted from frozen leaves (15 mm in length) and submitted to immunoblotting, as described previously (Vazquez-Flota and De Luca, 1998). TDC, D4H, and DAT antigens were decorated with the polyclonal antisera H95 (Fernandez et al., 1989), D4H-ab (Vazquez-Flota and De Luca, 1998), and affinity-purified DAT antibody (St-Pierre et al., 1998), respectively.

Procedures for the isolation, electrophoresis, and blotting of RNA, as well as the conditions for hybridization, posthybridization washes, and autoradiography, have been reported elsewhere (Vazquez-Flota and De Luca, 1998). *tdc*, *str1*, *d4h*, and *dat* transcripts were hybridized to

clones TDC-5 (De Luca et al., 1989), *str1* cDNA clone (McKnight et al., 1990), cD4H-3A (Vazquez-Flota et al., 1997), and pBSDAT3 (see above), respectively.

ACKNOWLEDGMENTS

We thank Dwight Beebe for access to the Olympus BH-2 microscope. We also thank Sylvain Lebeurier for maintenance of plants. This work was supported by the Natural Sciences and Engineering Research Council of Canada and Le Fonds pour la Formation de Chercheurs et l'Aide à la Recherche.

Received November 30, 1998; accepted March 9, 1999.

REFERENCES

Aerts, R., Gisi, D., De Carolis, E., De Luca, V., and Baumann, T.W. (1994). Methyl jasmonate vapor increases the developmentally controlled synthesis of alkaloids in *Catharanthus* and *Cinchona* seedlings. Plant J. **5,** 635–643.

Balsevich, J., and Bishop, G. (1989). Distribution of catharanthine, vindoline and 3′,4′-anhydrovinblastine in the aerial parts of some *Catharanthus roseus* plants and the significance thereof in relation to alkaloid production in cultured cells. In Primary and Secondary Metabolism of Plant Cell Cultures, W.G.W. Kurz, ed (Berlin: Springer-Verlag), pp. 149–153.

Balsevich, J., De Luca, V., and Kurz, W.G.W. (1986). Altered alkaloid pattern in dark grown seedlings of *Catharanthus roseus*. The isolation and characterization of 4-desacetoxyvindoline: A novel indole alkaloid and proposed precursor of vindoline. Heterocycles **24,** 2415–2421.

Bernier, G. (1988). The control of floral evocation and morphogenesis. Annu. Rev. Plant Physiol. Plant Mol. Biol. **39,** 175–219.

Bhadra, R., Vani, S., and Shanks, J.V. (1993). Production of indole alkaloids by selected hairy root lines of *Catharanthus roseus*. Biotechnol. Bioeng. **41,** 581–592.

Constabel, F., Gaudet-LaPrairie, P., Kurz, W.G.W., and Kutney, J.P. (1982). Alkaloid production in *Catharanthus roseus* cell cultures. XII. Biosynthetic capacity of callus from original explants and regenerated shoots. Plant Cell Rep. **1,** 139–142.

Dale, J.E. (1988). The control of leaf expansion. Annu. Rev. Plant Physiol. Plant Mol. Biol. **39,** 267–295.

De Carolis, E., and De Luca, V. (1993). Purification, characterization, and kinetic analysis of a 2-oxoglutarate–dependent dioxygenase involved in vindoline biosynthesis from *Catharanthus roseus*. J. Biol. Chem. **268,** 5504–5511.

De Carolis, E., Chan, F., Balsevich, J., and De Luca, V. (1990). Isolation and characterization of a 2-oxoglutarate dependent dioxygenase involved in the second-to-last step in vindoline biosynthesis. Plant Physiol. **94,** 1323–1329.

De Luca, V. (1993). Enzymology of indole alkaloid biosynthesis. In Methods in Plant Biochemistry, Enzymes of Secondary Metabolism, P.J. Lea, ed (London: Academic Press), pp. 345–368.

De Luca, V., Balsevich, J., and Kurz, W.G.W. (1985). Acetyl coenzyme A:deacetylvindoline *O*-acetyltransferase, a novel enzyme from *Catharanthus*. J. Plant Physiol. **121,** 417–428.

De Luca, V., Balsevich, J., Tyler, R.T., Eilert, U., Panchuk, B.D., and Kurz, W.G.W. (1986). Biosynthesis of indole alkaloids: Developmental regulation of the biosynthetic pathway from tabersonine to vindoline in *Catharanthus roseus*. J. Plant Physiol. **125,** 147–156.

De Luca, V., Balsevich, J., Tyler, R.T., and Kurz, W.G.W. (1987). Characterization of a novel *N*-methyltransferase (NMT) from *Catharanthus roseus* plants. Detection of NMT and other enzymes of the indole alkaloid biosynthetic pathway in different cell suspension culture systems. Plant Cell Rep. **6,** 458–461.

De Luca, V., Alvarez Fernandez, J., Campbell, D., and Kurz, W.G.W. (1988). Developmental regulation of enzymes of indole alkaloid biosynthesis in *Catharanthus roseus*. Plant Physiol. **86,** 447–450.

De Luca, V., Marineau, C., and Brisson, N. (1989). Molecular cloning and analysis of cDNA encoding a plant tryptophan decarboxylase: Comparison with animal dopa decarboxylases. Proc. Natl. Acad. Sci. USA **86,** 2582–2586.

Dethier, M., and De Luca, V. (1993). Partial purification of an *N*-methyltransferase involved in vindoline biosynthesis in *Catharanthus roseus*. Phytochemistry **32,** 673–678.

Deus-Neumann, B., Stöckigt, J., and Zenk, M.H. (1987). Radioimmunoassay for the quantitative determination of catharanthine. Planta Med. **53,** 184–188.

Eilert, U., Nesbitt, L.R., and Constabel, F. (1985). Laticifers and latex in fruits of periwinkle, *Catharanthus roseus*. Can. J. Bot. **63,** 1540–1546.

Endo, T., Goodbody, A., and Misawa, M. (1987). Alkaloid production in root and shoot cultures of *Catharanthus roseus*. Planta Med. **53,** 479–482.

Facchini, P.J., and De Luca, V. (1995). Phloem-specific expression of tyrosine/dopa decarboxylase genes and the biosynthesis of isoquinoline alkaloids in opium poppy. Plant Cell **7,** 1811–1821.

Fahn, A. (1988). Secretory tissues in vascular plants. New Phytol. **108,** 229–257.

Fernandez, J.A., Owen, T.G., Kurz., W.G.W., and De Luca, V. (1989). Immunological detection and quantification of tryptophan decarboxylase in developing *Catharanthus roseus* seedlings. Plant Physiol. **91,** 79–84.

Frischknecht, P.M., Ulmer-Dufek, J., and Baumann, T.W. (1986). Purine alkaloid formation in buds and developing leaflets of *Coffea arabica*: Expression of an optimal defense strategy? Phytochemistry **25,** 613–616.

Hashimoto, T., and Yamada, Y. (1994). Alkaloid biogenesis: Molecular aspects. Annu. Rev. Plant Physiol. Plant Mol. Biol. **45,** 257–285.

Herr, J.M. (1971). A new clearing-squash technique for the study of ovule development in angiosperms. Am. J. Bot. **58,** 785–790.

Ibrahim, R.K., De Luca, V., Khouri, H., Latchinian, L., Brisson, L., and Charest, P.M. (1987). Enzymology and compartmentation of polymethylated flavonol glucosides in *Chrysosplenium americanum*. Phytochemistry **26,** 1237–1245.

Jackson, D. (1992). In situ hybridization in plants. In Molecular Plant Pathology: A Practical Approach, S.J. Gurr, M.J. McPherson, and D.J. Bowles, eds (Oxford, UK: IRL Press at Oxford University), pp. 163–174.

Keene, C.K., and Wagner, G.J. (1985). Direct demonstration of duvatrienediol biosynthesis in glandular heads of tobacco trichomes. Plant Physiol. **79,** 1026–1032.

Kutchan, T.M., Ayabe, S., Krueger, R.J., Coscia, E.M., and Coscia, C.J. (1983). Cytodifferentiation and alkaloid accumulation in cultured cells of *Papaver bracteatum*. Plant Cell Rep. **2,** 281–284.

Lindsey, K., and Yeoman, M.M. (1983). The relationship between growth rate, differentiation and alkaloid accumulation in cell cultures. J. Exp. Bot. **34,** 1055–1065.

Luijendijk, T.J.C., Vandermeijden, E., and Verpoorte, R. (1996). Involvement of strictosidine as a defensive chemical in *Catharanthus roseus*. J. Chem. Ecol. **22,** 1355–1366.

McCaskill, D., Gershenzon, J., and Croteau, R. (1992). Morphology and monoterpene biosynthetic capabilities of secretory cell clusters isolated from glandular trichomes of peppermint (*Mentha piperita* L.). Planta **187,** 445–454.

McKnight, T.D., Roessner, C.A., Devagupta, R., Scott, A.I., and Nessler, C.L. (1990). Nucleotide sequence of a cDNA encoding the vacuolar protein strictosidine synthase from *Catharanthus roseus*. Nucleic Acids Res. **18,** 4939.

Mersey, B.G., and Cutler, A.J. (1986). Differential distribution of specific indole alkaloids in leaves of *Catharanthus roseus*. Can. J. Bot. **64,** 1039–1045.

Nessler, C.L., and Mahlberg, P.G. (1977). Ontogeny and cytochemistry of alkaloidal vesicles in laticifers of *Papaver somniferum* L. (Papaveraceae). Am. J. Bot. **64,** 541–551.

Pasquali, G., Goddijn, O.J.M., De Waal, A., Verpoorte, R., Schilperoort, R.A., Hoge, J.H.C., and Memelink, J. (1992). Coordinated regulation of two indole alkaloid biosynthetic genes from *Catharanthus roseus* by auxin and elicitors. Plant Mol. Biol. **18,** 1121–1131.

Platt, K.A., and Thomson, W.W. (1992). Idioblast oil cells of avocado: Distribution, isolation, ultrastructure, histochemistry, and biochemistry. Int. J. Plant Sci. **153,** 301–310.

Postek, M.T., and Tucker, S.C. (1983). Ontogeny and ultrastructure of secretory oil cells in *Magnolia grandiflora* L. Bot. Gaz. **144,** 501–512.

Power, R., Kurz, W.G.W., and De Luca, V. (1990). Purification and characterization of acetylcoenzyme A:deacetylvindoline 4-*O*-acetyltransferase from *Catharanthus roseus*. Arch. Biochem. Biophys. **279,** 370–376.

Reinold, S., and Hahlbrock, K. (1997). In situ localization of phenylpropanoid biosynthetic mRNAs and proteins in parsley (*Petroselinum crispum*). Bot. Acta **110,** 431–443.

Robinson, T. (1974). Metabolism and function of alkaloids in plants. Science **184,** 430–435.

Robinson, T. (1981). The Biochemistry of Alkaloids, 2nd ed. (New York: Springer-Verlag).

St-Pierre, B., and De Luca, V. (1995). A cytochrome P-450 monooxygenase catalyzes the first step in the conversion of tabersonine to vindoline in *Catharanthus roseus*. Plant Physiol. **109,** 131–139.

St-Pierre, B., Laflamme, P., Alarco, A.-M., and De Luca, V. (1998). The terminal *O*-acetyltransferase involved in vindoline biosynthesis defines a new class of proteins responsible for coenzyme A–dependent acyl transfer. Plant J. **14,** 703–713.

Svoboda, G.H., and Blake, D.A. (1975). The phytochemistry and pharmacology of *Catharanthus roseus* (L.) G. Don. In The *Catharanthus* Alkaloids: Botany, Chemistry, Pharmacology and Clinical Uses, W.I. Taylor and N.R. Farnsworth, eds (New York: Marcel Dekker Inc.), pp. 45–83.

Sylvester, A.W., Smith, L., and Freeling, M. (1996). Acquisition of identity in the developing leaf. Annu. Rev. Cell Dev. Biol. **12,** 257–304.

Toivonen, L., Balsevich, J., and Kurz, W.G.W. (1989). Indole alkaloid production by hairy root cultures of *Catharanthus roseus*. Plant Cell Tissue Organ Cult. **18,** 79–93.

van der Heijden, R., Verpoorte, R., and Ten Hoopen, H.J.G. (1989). Cell and tissue cultures of *Catharanthus roseus* (L.) G. Don: A literature survey. Plant Cell Tissue Organ Cult. **18,** 231–280.

Vazquez-Flota, F., and De Luca, V. (1998). Developmental and light regulation of desacetoxyvindoline 4-hydroxylase in *Catharanthus roseus* (L.) G. Don. Plant Physiol. **117,** 1351–1361.

Vazquez-Flota, F., De Carolis, E., Alarco, A.-M., and De Luca, V. (1997). Molecular cloning and characterization of desacetoxyvindoline-4-hydroxylase, a 2-oxoglutarate–dependent dioxygenase involved in the biosynthesis of vindoline in *Catharanthus roseus* (L.) G. Don. Plant Mol. Biol. **34,** 935–948.

von Arnim, A., and Deng, X.W. (1996). Light control of seedling development. Annu. Rev. Plant Physiol. Plant Mol. Biol. **47,** 215–243.

Weeks, W.W., and Bush, L.P. (1974). Alkaloid changes in tobacco seeds during germination. Plant Physiol. **53,** 73–75.

Westekemper, P., Wieczorek, U., Gueritte, F., Langlois, N., Langlois, Y., Potier, P., and Zenk, M.H. (1980). Radioimmunoassay for the determination of the indole alkaloid vindoline in *Catharanthus*. Planta Med. **39,** 24–37.

Yoder, L.R., and Mahlberg, P.G. (1976). Reactions of alkaloid and histochemical indicators in laticifers and specialized parenchyma cells of *Catharanthus roseus* (Apocynaceae). Am. J. Bot. **63,** 1167–1173.